Letter

Ballistic magnetotransport in graphene

Ke Wang [*] and T. A. Sedrakyan [†]
Department of Physics, University of Massachusetts, Amherst, Massachusetts 01003, USA

(Received 15 October 2021; revised 16 February 2022; accepted 17 March 2022; published 28 March 2022)

We report that a perpendicular magnetic field introduces an anomalous interaction correction, $\delta\sigma$, to the static conductivity of doped graphene in the ballistic regime. The correction implies that the magnetoresistance, $\delta\rho_{xx}$ scales inversely with temperature $\delta\rho_{xx}(T)\propto 1/T$ in a parametrically large interval. When the disorder is scalarlike, the $\propto 1/T$ behavior is the leading contribution in the crossover between diffusive regime exhibiting weak localization and quantum magnetooscillations. The behavior originates from the field-induced breaking of the chiral symmetry of Dirac electrons around a single valley. The result is specific for generic two-dimensional Dirac materials which deviate from the half-filling. We conclude by proposing magnetotransport experiments, which have the capacity to detect the nature of impurities and defects in high-mobility Dirac monolayers such as recently fabricated ballistic graphene samples.

DOI: 10.1103/PhysRevB.105.L121114

Introduction. Two well-established regimes characterize low-temperature magnetoresistance in a two-dimensional metallic system: Weak localization [1,2] (WL) and Shubnikov–de Haas (SdH) oscillations. WL dominates in the low field limit $\omega_0\tau < (k_F L)^{-1}$. Here ω_0 is the cyclotron-frequency, τ is the impurity scattering time, and $L = v_F\tau$ is the mean free path. This regime is reached when the magnetic flux threading the area $L^2/2$ is smaller than the flux quantum [3,4]. In the high field limit $\omega_0\tau > 1$, the spectrum is fully quantized into the Landau levels, and SdH oscillations become the dominating effect. The crossover between two limits is $(k_F L)^{-1} < \omega_0\tau < 1$, where the magnetic field B is nonquantizing. In this regime, the electron-electron interactions are believed to play a significant role [5]. Namely, the interaction correction to the conductivity induce the B dependence in the resistivity via the relation,

$$\delta\rho_{\rm int} \simeq \rho_0^2\left(\omega_0^2\tau^2 - 1\right)\delta\sigma_{\rm int}. \tag{1}$$

Here ρ_0 is the Drude resistivity and $\delta\sigma_{\rm int}$ is the interaction correction to the longitudinal conductivity.

At the nonquantizing regime, magnetoresistance in the doped graphene has been widely studied in experiments [6–10] in the last decade while theoretical investigations are still absent. One may expect that the B dependence in $\delta\rho_{\rm int}$ is simply product of $\rho^2\omega_0^2\tau^2$ and zero field performance in $\delta\sigma_{\rm int}$. However, it is not the complete story the nonquantizing field on Dirac electrons has nontrivial effects on Friedel oscillations (FO) [11] and many-body physics [12].

In this letter, we report that $\delta\sigma_{\rm int}$ itself can carry field-dependent corrections and thus leads to nontrivial magnetoresistance in graphene. In the ballistic regime $T\tau > 1$ of the doped graphene [10,13], we find

$$\delta\sigma_{\rm int} \simeq \lambda_0\frac{e^2\tau}{\pi}\left(tT - p\frac{\omega_0^2}{48T}\right). \tag{2}$$

Here λ_0 is the dimensionless interaction parameter, and t, p are dimensionless parameters determined by the disorder potential. Information about t and p can be extracted from the zero-bias anomaly [12,14] of tunneling density of states. The correction is present in a wide parameter range, where $\max(\omega_0, \tau^{-1}) < T < E_F$. Here E_F is the Fermi energy. From Eq. (1), the field-dependent correction to the resistivity reads [15],

$$\delta\rho_{\rm int}(B) - \delta\rho_{\rm int}(0) \simeq \lambda_0\omega_0^2\frac{e^2\tau^2\rho_0^2}{\pi}\left(tT\tau + \frac{p}{48T\tau}\right). \tag{3}$$

Temperature dependence of magnetoresistance in Eq. (3) highly depends on the ratio, p/t, of two disorder parameters that will be defined below. Generally, the ratio p/t can be any real number larger than $-1/2$. One prominent case is the scalarlike disorder potential, for which p/t is $\to +\infty$. To ensure the second term is not always subleading, we will focus on $p/t > 1$, where the disorder can be regarded as a perturbation around a scalarlike potential. When $1 < T\tau < \sqrt{p/t}$, the temperature dependence in magnetoresistance becomes reciprocal instead of being linear. Therefore, the parabolic curve in magnetoresistance becomes more flattened when T increases. See Fig. 1. Below, we present a qualitative explanation of the observed effect.

Qualitative discussion. Coherent scatterings off Friedel oscillations of electron density at distances $r \gg k_F^{-1}$ from an impurity renormalize the transport relaxation time. The coherent scattering is illustrated in Fig. 2. This process, leads to non-trivial temperature dependence[16,17] in $\delta\sigma_{\rm int}$. In two-dimensional electron gas, $\delta\sigma_{\rm int}$ is $\sim T\tau$ in the ballistic limit $T\tau > 1$ and $\sim\ln(T\tau)$ in the diffusive limit $T\tau < 1$.

The Dirac nature of electrons in graphene [18–36] can enrich the process of coherent scatterings because of the Berry

[*]kewang@umass.edu
[†]tsedrakyan@umass.edu

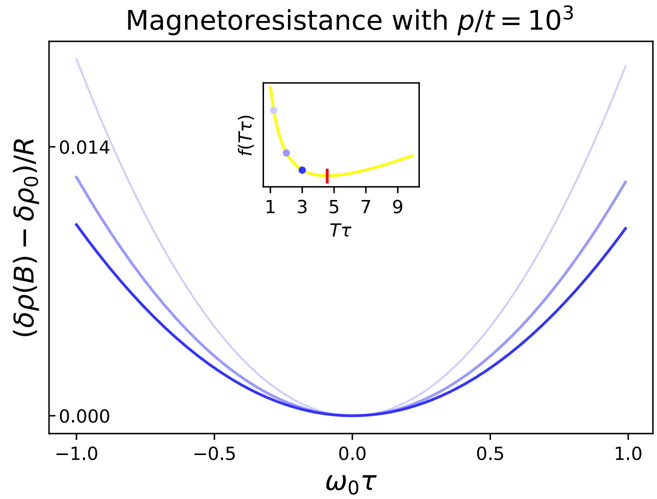

FIG. 1. Magnetoresistance, $[\delta\rho_{\text{int}}(B) - \delta\rho_{\text{int}}(0)]/R$, is plotted versus the dimensionless variable $\omega_0\tau$. The sign of $\omega_0\tau$ indicates the direction of the magnetic field and $R \equiv \lambda_0 e^2\rho_0^2/\pi$. Each curve correspond to the resistance plotted at a corresponding temperature shown by (blue) dots in the inset. From light to dark curves, the temperature is increasing while the curvature is decreasing. Values of temperature are pointed out in the inset. The inset depicts the function $f(T\tau) = tT\tau + p/48T\tau$ from Eq. (3). The (red) vertical bar locates the minimum of the function.

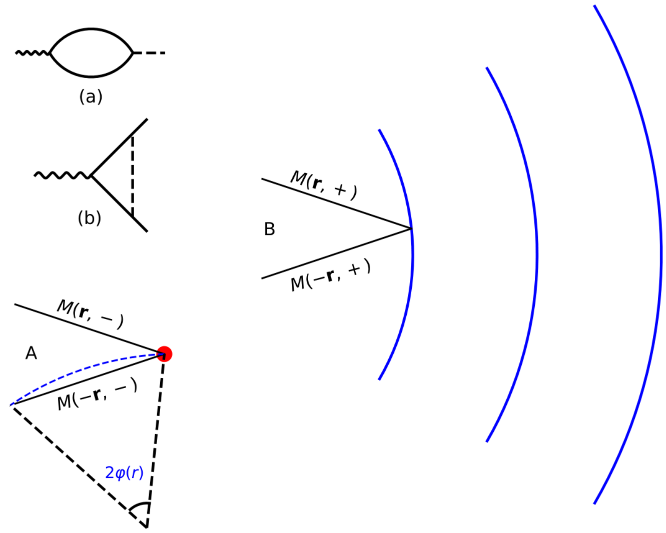

FIG. 2. Coherent scatterings between A and B paths: A is the path of backscattering off an impurity while B is the path when electrons hit the Friedel oscillations (or modulation of density matrix introduced by impurities), presented by blue curves. In the presence of a magnetic field, the path is curved, shown by the dashed arc. The angle of the arc is $2\varphi(r) = \omega_0 r/v_F$. Due to the Dirac nature of electrons, each propagator carries a matrix M. The inset plots two types of backscatterings off an impurity: (a) the loop type that creates Friedel oscillations. (b) the vertex type that creates correction to the density matrix.

phase π and chiral symmetry of Dirac electrons. Note that backscatterings off a single impurity can be classified into two types of Feynman diagrams. The first one is a loop type, giving Friedel oscillations. See inset (a) in Fig. 2. Here, the Berry phase π of Dirac electron leads to a faster decaying FO [37]. The second one is a vertex type diagram, yielding the correction to the density matrix. See inset (b) of Fig. 2. Here, the matrix structure of Dirac electron induces sensitivity of the vertex correction to the nature of disorder [14]. Two properties together lead to the well-known result that the temperature dependence in the conductivity in the ballistic limit is still $\sim T\tau$ but very sensitive to the disorder [37]. Importantly, if the disorder is scalarlike, the leading temperature behavior $\sim T\tau$ vanishes.

The presence of a weak magnetic field changes the scenario for both backscatterings in (a) and (b) from the inset of Fig. 2. The persistent FO emerges from loop correction [11],

$$\delta n(r) = \frac{gk_F}{2\pi^2 v_F r^2}\left[\frac{1}{k_F r}\cos\left(2k_F r - \frac{r^3}{12k_F l^4}\right) + 2\varphi^2(r)\sin\left(2k_F r - \frac{r^3}{12k_F l^4}\right)\right]. \tag{4}$$

Here the parameter g is defined in terms of the impurity potential, $\hat{V}_{\mathbf{r}}$, as $g = \text{tr}\int d^2r\hat{V}_{\mathbf{r}}/4$, $\varphi(r) = \omega_0 r/2v_F$ and l is the magnetic length. The $\varphi(r)$ is the half of the angle of the arc, corresponding to the Dirac electron traveling from $\mathbf{0}$ to $\mathbf{r}$ in a weak magnetic field. See Fig. 2. The value $\varphi(r)$ reflects the strength of chiral symmetry breaking semiclassically[11,38]. A similar correction also emerges for the vertex correction [12]. To evaluate the effect of the magnetic field on other physical processes [39] for Dirac electrons, employing the chiral-symmetry breaking phase $\varphi(r)$ could be essential as it could lead to novel observable effects.

As the next step, we will consider the transport relaxation time and see that the incorporation of $\varphi^2(r)$ into the estimate of the relaxation time can generate the correction in Eq. (2). It will help us to qualitatively extract the temperature behavior of magnetoconductivity from its relation to the transport time [40].

At first, let us estimate the relaxation time at zero-field, where a linear temperature dependence emerges:

$$\frac{1}{\tau} = \int\frac{d\theta}{2\pi}(1-\cos\theta)|f_0 + f_1(\theta)|^2. \tag{5}$$

Here f_0 and f_1 are, respectively, the scattering amplitudes off impurities and impurity-induced potentials. In the absence of the magnetic field, according to Refs. [17] and [41], the function f_1 can be cast as an integral $f_1(\theta) = \int drF(r)$ and

$$F(r) = -\lambda_0 g\int_0^{+\infty} dr\frac{r_T}{\sinh r/r_T}\sin(2k_F r)J_0(qr). \tag{6}$$

Here $r_T = v_F/(2\pi T)$ is the thermal length, $|q| = 2k_F\sin\theta/2$ and J_0 is the zero Bessel function. The coefficient λ_0 is the dimensionless interaction parameter and the main contribution to Eq. (5) comes from the region $\theta\sim\pi$. One can expand $\theta = \pi + \delta\theta$ and $q \simeq 2k_F - k_F\delta\theta^2$. The condition $k_F\delta\theta^2 r_T \sim 1$ translates into $\delta\theta \sim (k_F r_T)^{-1/2}$. With the asymptotic expression

of the Bessel function, the power counting in the integral becomes $r^{-3/2}$ when $r < r_T$. When $\delta\theta < (k_F r_T)^{-1/2}$, the integral in Eq. (6), gives $\sim(k_F r_T)^{-1/2}$. Thus the integral in Eq. (5) is estimated by $(k_F r_T)^{-1}$. This indicates that the interaction correction to τ is proportional to T and the corresponding correction to $\delta\sigma_{\rm int}$ is also linear in T.

In the presence of a magnetic field, the trajectories of electrons are curved, and the chiral symmetry of Dirac electrons is broken. Thus the suppressed backscattering is enhanced by the magnetic field. The incorporation of the symmetry-breaking effect leads to a field-dependent correction to the scattering amplitude. Namely, $f_1 \to f_1 + \delta f_1$ and δf_1 is given by $\int drF(r)\varphi^2(r)$. Here $\varphi^2(r)$ changes power counting to $r^{1/2}$ and the integral gives $\sim\omega_0^2(k_F r_T)^{3/2}$. The θ integral remains the same. Thus the field-dependent corrections to τ and $\delta\sigma_{\rm int}$ are proportional to $\omega_0^2 T^{-1}$.

Below, we rigorously trace the current-current correlation function to derive the temperature dependence in $\delta\sigma_{\rm int}$.

Magnetoconductivity from Kubo formula. The static conductivity can be evaluated from the current-current correlation function [40]. Namely, $\sigma_{\alpha,\beta} = \lim_{\omega\to 0}\frac{i}{\omega}\Pi_{\alpha,\beta}(\omega)$. Here the $\Pi_{\alpha,\beta}(\omega)$ is obtained by taking analytic continuation of current-current correlation function $\Pi_{\alpha,\beta}(i\Omega_n)$ via $i\Omega_n \to \omega$, $\Pi_{\alpha,\beta}(i\Omega_n) = \int_0^{1/T} d\tau \langle T_\tau \hat{j}_\alpha(\tau)\hat{j}_\beta(0)\rangle e^{i\Omega_n\tau}$ Here $\hat{j}_\alpha(\tau)$, $\alpha = 1, 2$, is the current operator at imaginary time τ, $\omega_n = 2\pi T n$ is the bosonic Matsubara frequency and $i\Omega_n \to \omega$ represents the analytic continuation.

At finite doping, one can treat impurity and interaction potential as the perturbation to $\hat{H}_0$. Here H_0 is the Dirac Hamiltonian coupled to the $U(1)$ gauge field,

$$\hat{H}_0 = v_F \int d^2\mathbf{r}\hat{\Psi}^\dagger(\mathbf{r})[\hat{\Sigma}_\alpha(-i\partial^\alpha + eA^\alpha)]\hat{\Psi}(\mathbf{r}). \quad (7)$$

Here α is summed in x and y, v_F is the Fermi velocity, $\hat{\Psi} = (\hat{\psi}_{AK}, \hat{\psi}_{BK}, \hat{\psi}_{BK'}, \hat{\psi}_{AK'})$ is the four-component fermion operator and $\hat{\Sigma}_{x,y} = \hat{\tau}_z \otimes \hat{\sigma}_{x,y}$, where $\hat{\tau}_z$ is the third Pauli matrix acting in K, K' space and $\hat{\sigma}_{x,y}$ are Pauli matrices acting in the space of A, B sublattices. The gauge field is adopted by $\mathbf{A} = (-eBy, 0)$.

Now, we consider the Gaussian-correlated potential. Meanwhile, the symmetry-allowed disorder potential is described by five parameters [42–44], namely,

$$\langle \hat{V}_\mathbf{r} \otimes \hat{V}_{\mathbf{r}'}\rangle = \delta_{\mathbf{r},\mathbf{r}'}\big[\gamma_0 \hat{I} \otimes \hat{I} + g_i^m \hat{Q}_m^i \otimes \hat{Q}_m^i\big]. \quad (8)$$

Here $\hat{V}_\mathbf{r}$ is the impurity potential and the bracket $\langle\ldots\rangle$ is the average over impurity distributions. $\hat{I}$ is the identity matrix. Here $\hat{Q}_m^i = \hat{\Sigma}_m\hat{\Lambda}_i$ and $\hat{\Sigma}_z = \hat{\tau}_0 \otimes \hat{\sigma}_z$, $\hat{\Lambda}_x = \hat{\tau}_x \otimes \hat{\sigma}_z$, $\hat{\Lambda}_y = \hat{\tau}_y \otimes \hat{\sigma}_z$, $\hat{\Lambda}_z = \hat{\tau}_z \otimes \hat{\sigma}_0$. We adpot the notation from Ref. [42], $g_z^z = \gamma_z$, $g_z^{x,y} = \gamma_\perp$, $g_{x,y}^z = \beta_z$ and $g_{x,y}^{x,y} = \beta_\perp$. Effectively, γ_0 represents the square of the strength of static electric potential averaged over the A/B sublattice. Parameters β_z and $\beta_\perp$ introduce the intervalley scatterings while $\gamma_\perp$ introduces the hopping between A and B sublattices. The parameter γ_z creates a chemical potential difference between the A/B sublattices. To clarify terminology, we refer to the impurity potential from γ_0 term as the scalar potential while all other terms in the potential as nondiagonal.

To illustrate coherent scattering quantitatively, we use the semiclassical expression of Dirac propagators in the real space [12], $\langle G(\mathbf{r}, \omega)\rangle \sim e^{i{\rm sgn}(\omega)\Phi_0(r) - r/(2\tau v_F)} M(r, {\rm sgn}(\omega))/k_F r$. Here $\Phi_0(r)$ is the phase including both $k_F r$ and the magnetic phase [45,46]. The form of matrix M shows that chiral-symmetry is broken in each valley but it is preserved in the Brillouin zone [12]. The field-dependent part in M reads, $M - M_0 \simeq -\varphi^2(r)\hat{I}/2 - i{\rm sgn}(\omega)\varphi(r)\hat{\Sigma}_z$. Here M_0 is the value of matrix M in the absence of field and $\hat{I}$ is the identity matrix.

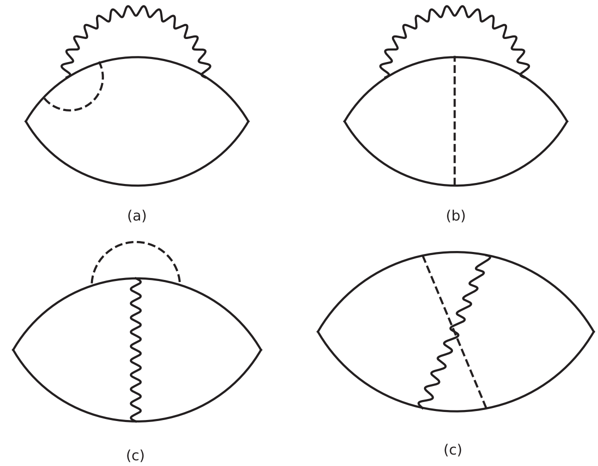

FIG. 3. Feynman diagrams giving leading field-dependent corrections to the longitudinal static conductivity. Solid lines represent the Feynman propagators. Dashed lines are the static impurities, while the wavy lines represent the electron-electron interactions.

Applying perturbations, one finds that a series of Feynman diagrams led to dominant contributions to the conductivity. Up to the lowest orders of the impurity potential and interactions, we find that the diagrams in Fig. 3 give the leading field-dependent corrections to the longitudinal and static conductivity, $\delta\sigma_{xx}$. Namely, these are diagrams that contain vertex corrections [12], while others in the same order of perturbation theory are subleading.

The exact expression corresponding diagrams in Fig. 3 can be simplified. In the leading in $(T\tau)^{-1}$ order, and upon neglecting highly-oscillatory $\sim\exp i2k_F r$ terms, one arrives at a short expression for the conductivity correction [47],

$$\delta\sigma_{xx} \simeq -\lambda_0 \frac{e^2\tau}{\pi^2\alpha_{\rm tr}} \int_0^{E_F} d\Omega \frac{d}{d\Omega}\Big(\Omega\coth\frac{\Omega}{2T}\Big){\rm Im}I(\Omega). \quad (9)$$

Here the function $I(\Omega)$ is expressed by the integral, $I(\Omega) = \int y^{-1}dy(2p'\varphi^2(y) + t')e^{2i(\Omega+i\tau)y/v_F}$, $\lambda_0 = k_F U_0/2\pi v_F$ is the dimensionless interaction constant at zero momentum. Parameters p' and t' are defined by $p' = \gamma_0 - \beta_z - \gamma_z$ and $t' = 2\gamma_z + 2\beta_z + \beta_\perp + \gamma_\perp$. The expression of $I(\Omega)$ originates from the coherent scatterings in Fig. 2. Notice the constant t' does not contain γ_0, while p', representing the enhancement of backscattering, depends on γ_0. For short-ranged and weak scatterers, the parameter $\alpha_{\rm tr}$ is found to be $\alpha_{\rm tr} = \gamma_0 + 4\beta_\perp + 2\gamma_\perp + 2\beta_z + \gamma_z$, determining the Drude conductivitvy in graphene [44].

The integration in the expression of ${\rm Im}I(\Omega)$ can be analytically performed, giving

$${\rm Im}I(\Omega) = \frac{\pi t}{2} + p\frac{(\omega_0\tau)^2}{4}\frac{\Omega\tau}{(1+\Omega^2\tau^2)^2}. \quad (10)$$

The zero-field part shares the same integration as in Ref. [17]. The linear T dependence in $\delta\sigma_{xx}$ at the zero field is obtained from the property, $\lim_{\Omega\to 0}\Omega\coth\Omega/2T \simeq 2T$. The sensitivity to the disorder potential in the zero-field limit, namely the sensitivity to parameter t, agrees well with the result in Ref. [37].

The field-dependent correction in Eq. (9) mainly originates from the region $0 < \Omega < 2T$. In this region, one can linearize $\frac{d}{d\Omega}(\Omega\coth\frac{\Omega}{2T}) \simeq \Omega/3T$. Notice that the charateristic scale for Ω in Eq. (10) is $\sim\tau^{-1}$. The integral over Ω does not introduce extra temperature dependence. Thus the field-dependent correction $\delta\sigma_{xx}$ is $\sim\omega_0^2 T^{-1}$. Tracing the integral rigorously, one can obtain Eq. (2), where we define $t = t'/\alpha_{\rm tr}$ and $p = p'/\alpha_{\rm tr}$. Inverting the magnetoconductivity tensor gives us Eq. (3), which is the main result of the present work. The result is specific for Dirac electron and valid in a large parameter space when $\omega_0 < T < E_F$. In Ref. [47], we provide the comparison between the mechanism reported here and the hydrodynamics description [48–56], which is the recent focus of studies on the transport of graphene. We show in Ref. [47], that for the doped and ultraclean sample, the reported ballistic magnetotransport mechanism is the dominating effect when the temperature, T, within the logarithmic accuracy, lies in a parametrically large interval $(\frac{k_B}{\hbar\tau}) \lesssim T \lesssim (\frac{k_B}{\hbar\tau})[\frac{\hbar E_F\tau}{k_B\ln(\hbar E_F\tau/k_B)}]^{1/2}$ (from now on we restore $k_B/\hbar$ prefactor in the expression for T).

The present technological capabilities do not allow one to engineer the graphene samples with a given impurity type to the best of our knowledge. Therefore, the present theory allows extracting the information about the impurity in the sample from the magnetotransport measurement. Namely, upon fitting the temperature dependence of observed magnetoresistance with Eq. (3), one can extract the ratio of p/t. This helps to understand if the impurity in the given sample is mostly scalar type ($p/t \gg 1$) or mostly nondiagonal ($p/t \lesssim 1$).

Implications for experiments. The new magnetoresistance behavior can be observed in experiments, provided with two conditions on disorder: (1) The disorder in the sample should ensure the inequality, $p/t \gg 1$. (2) The sample should be clean enough so that the ballistic transport can be observed.

To ensure $p/t \gg 1$, the type of disorder in a sample needs to be primarily scalarlike. Namely, only a small portion of disorder potentials create intravalley scatterings $A \leftrightarrows B$, intervalley scatterings $K \leftrightarrows K'$, and different on-site chemical potentials on sublattices.

The ballistic transport sets a lower bound for temperature, $T > T_0 \equiv k_B/\hbar\tau$. Meanwhile, the temperature should be low enough so that the thermal effects and phonon effects do not defeat the quantum effects of electrons. Thus sample should be clean enough for T_0 to represent a low temperature. In the previous *magnetotransport* experiments, samples under consideration were not clean enough for the ballistic transport to be observed. For example, in Refs. [7] and [8], the mobility of sample is $\mu \sim 2\times 10^3$ cm/Vs and the transport time is $\tau \sim 100$ fs. The temperature T_0 is $T_0 \sim 500$ K. This is a high temperature where thermal, and phonon effects [57–62] are strong and dominating. Nowadays, a clean sample with highly mobile electrons can be fabricated. According to Ref. [63], the method of chemical vapor deposition on reusable copper can be used to fabricate the graphene device with a high mobility, $\mu \sim 3.5\times 10^5$ cm/Vs. The subsequent work [13] shows that the electron mobility can be enhanced to be $\mu \sim 3\times 10^6$ cm/Vs together with the observation of ballistic transport at 1.7 K. These recent techniques may allow one to study the magnetoresistance of the doped graphene in the ballistic regime [64,65]. In this regard, the predicted phenomenon in this letter can be observed.

Acknowledgments. We are grateful to M. E. Raikh for valuable discussions. The research was supported by startup funds from the University of Massachusetts, Amherst.

[1] S. Hikami, A. I. Larkin, and Y. Nagaoka, Spin-orbit interaction and magnetoresistance in the two dimensional random system, Prog. Theor. Phys. **63**, 707 (1980).

[2] B. L. Altshuler, D. Khmel'nitzkii, A. I. Larkin, and P. A. Lee, Magnetoresistance and Hall effect in a disordered two-dimensional electron gas, Phys. Rev. B **22**, 5142 (1980).

[3] M.I. Dyakonov, Magnetoconductance due to weak localization beyond the diffusion approximation: The high-field limit, Solid State Commun. **92**, 711 (1994).

[4] A. Cassam-Chenai and B. Shapiro, Two dimensional weak localization beyond the diffusion approximation, J. Phys. I France **4**, 1527 (1994).

[5] T. A. Sedrakyan and M. E. Raikh, Crossover from Weak Localization to Shubnikov–de Haas Oscillations in a High-Mobility 2D Electron Gas, Phys. Rev. Lett. **100**, 106806 (2008).

[6] A. A. Kozikov, A. K. Savchenko, B. N. Narozhny, and A. V. Shytov, Electron-electron interactions in the conductivity of graphene, Phys. Rev. B **82**, 075424 (2010).

[7] B. Jouault, B. Jabakhanji, N. Camara, W. Desrat, C. Consejo, and J. Camassel, Interplay between interferences and electron-electron interactions in epitaxial graphene, Phys. Rev. B **83**, 195417 (2011).

[8] J. Jobst, D. Waldmann, I. V. Gornyi, A. D. Mirlin, and H. B. Weber, Electron-Electron Interaction in the Magnetoresistance of Graphene, Phys. Rev. Lett. **108**, 106601 (2012).

[9] B. Jabakhanji, D. Kazazis, W. Desrat, A. Michon, M. Portail, and B. Jouault, Magnetoresistance of disordered graphene: From low to high temperatures, Phys. Rev. B **90**, 035423 (2014).

[10] K. Gopinadhan, Y. J. Shin, R. Jalil, T. Venkatesan, A. K. Geim, A. H. C. Neto, and H. Yang, Extremely large magnetoresistance in few-layer graphene/boron–nitride heterostructures, Nat. Commun. **6**, 8337 (2015).

[11] K. Wang, M. E. Raikh, and T. A. Sedrakyan, Persistent friedel oscillations in graphene due to a weak magnetic field, Phys. Rev. B **103**, 085418 (2021).

[12] K. Wang, M. E. Raikh, and T. A. Sedrakyan, Interaction effects in graphene in a weak magnetic field, Phys. Rev. B **104**, L161102 (2021).

[13] L. Banszerus, M. Schmitz, S. Engels, M. Goldsche, K. Watanabe, T. Taniguchi, B. Beschoten, and C. Stampfer, Ballistic transport exceeding 28μm in cvd grown graphene, Nano Lett. **16**, 1387 (2016).

[14] E. Mariani, L. I. Glazman, A. Kamenev, and F. von Oppen, Zero-bias anomaly in the tunneling density of states of graphene, Phys. Rev. B **76**, 165402 (2007).

[15] G. Zala, B. N. Narozhny, and I. L. Aleiner, Interaction corrections to the Hall coefficient at intermediate temperatures, Phys. Rev. B **64**, 201201(R) (2001).

[16] A. Gold and V. T. Dolgopolov, Temperature dependence of the conductivity for the two-dimensional electron gas: Analytical results for low temperatures, Phys. Rev. B **33**, 1076 (1986).

[17] G. Zala, B. N. Narozhny, and I. L. Aleiner, Interaction corrections at intermediate temperatures: Longitudinal conductivity and kinetic equation, Phys. Rev. B **64**, 214204 (2001).

[18] Y. W. Tan, Y. Zhang, H. L. Stormer, and P. Kim, Temperature dependent electron transport in graphene, Eur. Phys. J.: Spec. Top. **148**, 15 (2007).

[19] K. I. Bolotin, K. J. Sikes, Z. Jiang, M. Klima, G. Fudenberg, J. Hone, P. Kim, and H. L. Stormer, Ultrahigh electron mobility in suspended graphene, Solid State Commun. **146**, 351 (2008).

[20] K. Nomura and A. H. MacDonald, Quantum Transport of Massless Dirac Fermions, Phys. Rev. Lett. **98**, 076602 (2007).

[21] S. Das Sarma, E. H. Hwang, and W. K. Tse, Many-body interaction effects in doped and undoped graphene: Fermi liquid versus non-Fermi liquid, Phys. Rev. B **75**, 121406(R) (2007).

[22] K. I. Bolotin, K. J. Sikes, J. Hone, H. L. Stormer, and P. Kim, Temperature-Dependent Transport in Suspended Graphene, Phys. Rev. Lett. **101**, 096802 (2008).

[23] A. H. Castro Neto, F. Guinea, N. M. R. Peres, K. S. Novoselov, and A. K. Geim, The electronic properties of graphene, Rev. Mod. Phys. **81**, 109 (2009).

[24] S. Das Sarma, S. Adam, E. H. Hwang, and E. Rossi, Electronic transport in two-dimensional graphene, Rev. Mod. Phys. **83**, 407 (2011).

[25] M. O. Goerbig, Electronic properties of graphene in a strong magnetic field, Rev. Mod. Phys. **83**, 1193 (2011).

[26] V. N. Kotov, B. Uchoa, V. M. Pereira, F. Guinea, and A. H. Castro Neto, Electron-electron interactions in graphene: Current status and perspectives, Rev. Mod. Phys. **84**, 1067 (2012).

[27] S. Maiti and T. A. Sedrakyan, Composite fermion state of graphene as a Haldane-Chern insulator, Phys. Rev. B **100**, 125428 (2019).

[28] C. Dutreix, H. González-Herrero, I. Brihuega, M. I. Katsnelson, C. Chapelier, and V. T. Renard, Measuring the berry phase of graphene from wavefront dislocations in friedel oscillations, Nature (London) **574**, 219 (2019).

[29] D. Pan, H. Xu, and F. J. García de Abajo, Anomalous Thermodiffusion of Electrons in Graphene, Phys. Rev. Lett. **125**, 176802 (2020).

[30] B. N. Narozhny, I. V. Gornyi, and M. Titov, Hydrodynamic collective modes in graphene, Phys. Rev. B **103**, 115402 (2021).

[31] G. Wagner, D. X. Nguyen, and S. H. Simon, Transport properties of multilayer graphene, Phys. Rev. B **101**, 245438 (2020).

[32] S. A. Mikhailov, Nonperturbative quasiclassical theory of graphene photoconductivity, Phys. Rev. B **103**, 245406 (2021).

[33] T. Zhu, M. Antezza, and J. S. Wang, Dynamical polarizability of graphene with spatial dispersion, Phys. Rev. B **103**, 125421 (2021).

[34] M. Kamada, V. Gall, J. Sarkar, M. Kumar, A. Laitinen, I. Gornyi, and P. Hakonen, Strong magnetoresistance in a graphene Corbino disk at low magnetic fields, Phys. Rev. B **104**, 115432 (2021).

[35] B. Real, O. Jamadi, M. Milićević, N. Pernet, P. St-Jean, T. Ozawa, G. Montambaux, I. Sagnes, A. Lemaître, L. Le Gratiet, A. Harouri, S. Ravets, J. Bloch, and A. Amo, Semi-Dirac Transport and Anisotropic Localization in Polariton Honeycomb Lattices, Phys. Rev. Lett. **125**, 186601 (2020).

[36] P. Sharma, A. Principi, and D. L. Maslov, Optical conductivity of a dirac-fermi liquid, Phys. Rev. B **104**, 045142 (2021).

[37] V. V. Cheianov and V. I. Fal'ko, Friedel Oscillations, Impurity Scattering, and Temperature Dependence of Resistivity in Graphene, Phys. Rev. Lett. **97**, 226801 (2006).

[38] G. W. Semenoff, Chiral symmetry breaking in graphene, Phys. Scr. **2012**, 014016 (2012).

[39] C. Faugeras, P. Kossacki, D. M. Basko, M. Amado, M. Sprinkle, C. Berger, W. A. de Heer, and M. Potemski, Effect of a magnetic field on the two-phonon raman scattering in graphene, Phys. Rev. B **81**, 155436 (2010).

[40] G. D. Mahan, *Many-Particle Physics* (Springer, Boston, 2000).

[41] T. A. Sedrakyan and M. E. Raikh, Magneto-Oscillations due to Electron-Electron Interactions in the ac Conductivity of a Two-Dimensional Electron Gas, Phys. Rev. Lett. **100**, 086808 (2008).

[42] I. L. Aleiner and K. B. Efetov, Effect of Disorder on Transport in Graphene, Phys. Rev. Lett. **97**, 236801 (2006).

[43] A. Altland, Low-Energy Theory of Disordered Graphene, Phys. Rev. Lett. **97**, 236802 (2006).

[44] P. M. Ostrovsky, I. V. Gornyi, and A. D. Mirlin, Electron transport in disordered graphene, Phys. Rev. B **74**, 235443 (2006).

[45] T. A. Sedrakyan, E. G. Mishchenko, and M. E. Raikh, Smearing of the Two-Dimensional Kohn Anomaly in a Nonquantizing Magnetic Field: Implications for Interaction Effects, Phys. Rev. Lett. **99**, 036401 (2007).

[46] T. A. Sedrakyan and M. E. Raikh, Interaction effects in a two-dimensional electron gas in a random magnetic field: Implications for composite fermions and the quantum critical point, Phys. Rev. B **77**, 115353 (2008).

[47] See Supplemental Material at http://link.aps.org/supplemental/10.1103/PhysRevB.105.L121114 for the detailed derivation of the static longitudinal conductivity from Kubo formula and the comparison of the reported mechanism and the hydrodymics in graphene.

[48] G. Yu. Vasileva, D. Smirnov, Yu. L. Ivanov, Yu. B. Vasilyev, P. S. Alekseev, A. P. Dmitriev, I. V. Gornyi, V. Yu. Kachorovskii, M. Titov, B. N. Narozhny, and R. J. Haug, Linear magnetoresistance in compensated graphene bilayer, Phys. Rev. B **93**, 195430 (2016).

[49] P. S. Alekseev, A. P. Dmitriev, I. V. Gornyi, V. Yu. Kachorovskii, B. N. Narozhny, and M. Titov, Counterflows in viscous electron-hole fluid, Phys. Rev. B **98**, 125111 (2018).

[50] B. N. Narozhny, I. V. Gornyi, and M. Titov, Anti-poiseuille flow in neutral graphene, Phys. Rev. B **104**, 075443 (2021).

[51] P. S. Alekseev, Negative Magnetoresistance in Viscous Flow of Two-Dimensional Electrons, Phys. Rev. Lett. **117**, 166601 (2016).

[52] P. S. Alekseev, A. P. Dmitriev, I. V. Gornyi, V. Yu. Kachorovskii, B. N. Narozhny, and M. Titov, Nonmonotonic magnetoresistance of a two-dimensional viscous electron-hole fluid in a confined geometry, Phys. Rev. B **97**, 085109 (2018).
[53] G. M. Gusev, A. S. Jaroshevich, A. D. Levin, Z. D. Kvon, and A. K. Bakarov, Viscous magnetotransport and gurzhi effect in bilayer electron system, Phys. Rev. B **103**, 075303 (2021).
[54] T. Scaffidi, N. Nandi, B. Schmidt, A. P. Mackenzie, and J. E. Moore, Hydrodynamic Electron Flow and Hall Viscosity, Phys. Rev. Lett. **118**, 226601 (2017).
[55] E. H. Hasdeo, J. Ekström, E. G. Idrisov, and T. L. Schmidt, Electron hydrodynamics of two-dimensional anomalous Hall materials, Phys. Rev. B **103**, 125106 (2021).
[56] A. Lucas and K. Chung Fong, Hydrodynamics of electrons in graphene, J. Phys.: Condens. Matter **30**, 053001 (2018).
[57] E. H. Hwang and S. Das Sarma, Acoustic phonon scattering limited carrier mobility in two-dimensional extrinsic graphene, Phys. Rev. B **77**, 115449 (2008).
[58] S. Fratini and F. Guinea, Substrate-limited electron dynamics in graphene, Phys. Rev. B **77**, 195415 (2008).
[59] D. L Nika and A. A. Balandin, Two-dimensional phonon transport in graphene, J. Phys.: Condens. Matter **24**, 233203 (2012).
[60] D. K. Efetov and P. Kim, Controlling Electron-Phonon Interactions in Graphene at Ultrahigh Carrier Densities, Phys. Rev. Lett. **105**, 256805 (2010).
[61] J. H. Seol, I. Jo, A. L. Moore, L. Lindsay, Z. H. Aitken, M. T. Pettes, X. Li, Z. Yao, R. Huang, D. Broido, N. Mingo, R. S. Ruoff, and L. Shi, Two-dimensional phonon transport in supported graphene, Science **328**, 213 (2010).
[62] A. Sedrakyan, A. Sinner, and K. Ziegler, Deformation of a graphene sheet: Interaction of fermions with phonons, Phys. Rev. B **103**, L201104 (2021).
[63] L. Banszerus, M. Schmitz, S. Engels, J. Dauber, M. Oellers, F. Haupt, K. Watanabe, T. Taniguchi, B. Beschoten, and C. Stampfer, Ultrahigh-mobility graphene devices from chemical vapor deposition on reusable copper, Sci. Adv. **1**, e1500222 (2015).
[64] X. Du, I. Skachko, and E. Y. Andrei, Towards ballistic transport in graphene, Int. J. Mod. Phys. B **22**, 4579 (2008).
[65] X. Du, I. Skachko, A. Barker, and E. Y. Andrei, Approaching ballistic transport in suspended graphene, Nat. Nanotechnol. **3**, 491 (2008).